

Optical sensors

A Self-Referencing Intensity-Based Fabry–Perot Cavity for Curvature Measurement

Susana Novais¹ , Susana O. Silva¹, and Orlando Frazão^{1,2}¹INESC TEC- Institute for Systems and Computer Engineering, Technology and Science, Porto 4169-007, Portugal²Department of Physics and Astronomy, Faculty of Sciences of University of Porto, Porto 4169-007, Portugal

Manuscript received July 26, 2019; revised August 19, 2019; accepted August 21, 2019. Date of publication August 26, 2019; date of current version October 4, 2019.

Abstract—In this article, a self-referencing intensity-based fiber optic sensor relying on the principle of Fabry–Perot interference is proposed and demonstrated to measure curvature. The sensor is manufactured producing an air bubble cavity between two sections of multimode fiber. By detecting optical power variations at specific wavelengths, it was possible to measure curvature, enabling this sensor as a self-referencing system. For this setup, the achieved curvature sensitivity was $0.561 \pm 0.014 \text{ dB/m}^{-1}$, with a correlation factor up to 0.997, within the measurement range of $0.0\text{--}0.8 \text{ m}^{-1}$. The proposed system has several features, including the self-referencing characteristic and its structure simplicity in terms of measuring procedure, making it a useful system.

Index Terms— Optical sensors, curvature, intensity-based sensor, self-referencing.

I. INTRODUCTION

Interferometric optical fiber sensors are based on the principle of optical interference for the measurement of chemical or physical properties. These sensors can be a great solution for sensing as they can exhibit great sensitivity, a wide dynamic range, multiplexing capacity, and low losses [1]. For many years, these sensors have been broadly studied due to their potential to be utilized in a wide range of applications. However, within the interferometers, the Fabry–Perot interferometer (FPI) is the most used, due to its optical characteristics [2], [3]. One of the first works relying on a fiber optic-based FPI sensor was reported in 1982, by Yoshino *et al.* [4]. Since then, a great and rapid evolution occurred in this field. This kind of sensors can be used to measure different physical parameters such as: refractive index [5], pressure [6], lateral load [7], magnetic field [8], displacement [9], and curvature [3], [10], [11].

There are several areas in which the measurement of the curvature parameter has special importance, such as: structural health monitoring, bridge and road construction, mechanical engineering, human posture detection, structural deformation [12]–[14], microelectro mechanical systems [15], and for monitoring smart and composite engineering structures, prosthetics designs, industrial metrology, robotics, and medical treatment [16]. The optical fiber curvature sensors has great advantages compared to electrical sensors, due to their high sensitivity and low maintenance costs, small size, small volume, corrosion resistance, high thermo-stability, high response speed, electromagnetic immunity, and capability of remote sensing—i.e., they have great potential to be used in curvature measurements [17], [18].

Several configurations have already been reported for curvature sensing. For instance, in 2013, a curvature and displacement sensing arrangement based on a fiber-optic micro-FPI was proposed [3]. This FPI was developed by applying arc discharges to a hollow core photonic crystal fiber. In 2014, a curvature sensor based on abrupt

tapered fiber joined with a micro-FP interferometer was reported [18]. In 2016, an FPI-based curvature sensor based on a capillary silica tube spliced between two single mode fibers was presented [11]. In 2017, an asymmetrical FPI fiber sensor for simultaneous measurement of curvature and temperature was demonstrated [19]. Later, a temperature insensitive directional bending sensor based on an eccentric-core fiber cascaded with an air cavity FPI was developed [20]. Recently, a curvature sensor based on the principle of FPI was reported, which was fabricated with a single-mode fiber (SMF), a ceramic tube, and double-cladding fiber [15]. The manufacturing process only required fiber cutting and the fiber fusion splicer.

In the present work, the development of an FPI air cavity made by splicing two sections of multimode fiber is proposed. It was designed as a simple setup based on two fiber Bragg gratings (FBGs), with the main objective of using them as two discrete optical sources in two distinct regions of the sensing head spectrum. The sensor was characterized for curvature and temperature measurements. The feature of self-referencing is also presented.

II. FABRICATION OF THE SENSING ELEMENT AND PRINCIPLE OF OPERATION

The sensing element used in this article is based on a fiber optic FPI. The FPI sensor was obtained by producing an air bubble between two sections of multimode fiber (MMF GIF625, supplied by Thorlabs, Newton, NJ, USA), having a diameter of 62.5 and 125 μm the core and cladding, respectively. The length of graded-index fiber between the SMF and the air bubble is $\sim 3 \text{ mm}$. The detailed process of fabrication is described in [7]. The technique used allows the fabrication of FPI sensors with different cavity lengths. These lengths are controlled through the successive electrical arcs that are applied to the MMF [7]. The schematic of the FPI sensor with a cavity length of 225 μm is shown on Fig. 1.

The operation mode of the sensor relies on excitation of higher order modes along the lead-in MMF section [21], [22] that it turn will illuminate the FPI cavity. The back-reflected light traveling through the MMF depends on the geometry of the microsphere. Then, a part

(S. O. Silva and O. Frazão contributed equally to this work.) Corresponding author: Susana Novais (e-mail: susana.novais@inesctec.pt).

Associate Editor: X. Shu.

Digital Object Identifier 10.1109/LSENS.2019.2937378

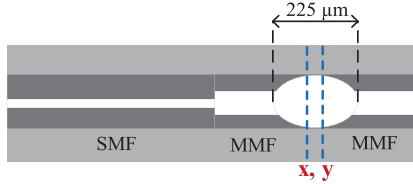


Fig. 1. Schematic of the FPI sensor.

of this light will be guided back by the SMF, since the acceptance angle acts as a filter [23]. When the FPI is subjected to curvature, the optical power variation as a function of wavelength is related to the excitation of the modes in the MMF section, and thus, it will influence the spectral behavior of the FPI. Interference between higher order modes is more affected by bending of the MMF section, while lower order modes are focused within a smaller area near the fiber core and are consequently less affected by the bending disturbance. Therefore, distinct MMF modes are excited by the light that is back-reflected from the FP cavity subjected to bending, thus creating different curvature sensitivities. For longer wavelengths (red shift), the FPI is sensitive to optical losses, whereas for smaller wavelengths (blue shift), the sensitivity to optical losses is residual.

III. CURVATURE SENSING

A. Experimental Setup and Calibration

A conventional system was used to observe the FPI spectral response in a typical reflection scheme. The purpose is to observe the pattern fringe change when is subjected to curvature and to analyze the wavelength peak variation within the full range of the broadband source.

In this case, the experimental setup relies on a broadband optical source centered at 1550 nm with 100 nm of bandwidth and an optical spectrum analyzer with a resolution of 0.01 dB. An optical circulator allows interrogation of the FPI in reflection.

The behavior of this structure as a curvature sensor was duly characterized. A section of optical fiber with a length 170 mm and having the FPI sensor in the middle was clamped between a fixed base and a 1-D translation stage. In this procedure, the curvature can be effortlessly calculated by using the formula [24]

$$C = \frac{1}{R} = \frac{2h}{h^2 + S^2} \quad (1)$$

where C , R , S , and h are curvature, curvature radius, half-distance between the two fixed points, and the bending displacement at the center of the FPI sensor, respectively. The bending displacement, h , was applied to the FPI via sequential $1 \times 10^3 \mu\text{m}$ displacements.

Fig. 2 shows the spectral behavior of the FP cavity to curvature. The red and black lines correspond to the curvature values of 0.0 and 0.76 m^{-1} , respectively. A zoom in of two distinct spectral regions is presented, namely at 1536 and 1554 nm, where different curvature sensitivities are clearly observed.

By analyzing the reflection spectra shown in Fig. 2, it is quite visible the fringe insensitivity to curvature at 1536 nm, while at 1554 nm it presents a clear sensitivity to the measured parameter. Therefore, by using these two wavelength-regions, it is possible to enable a self-referencing system.

For the self-referencing demonstration, an acquisition system such as the one shown in Fig. 3 was used. A broadband source with a 100 nm bandwidth is placed in port 1 of a 4-port optical circulator, while two

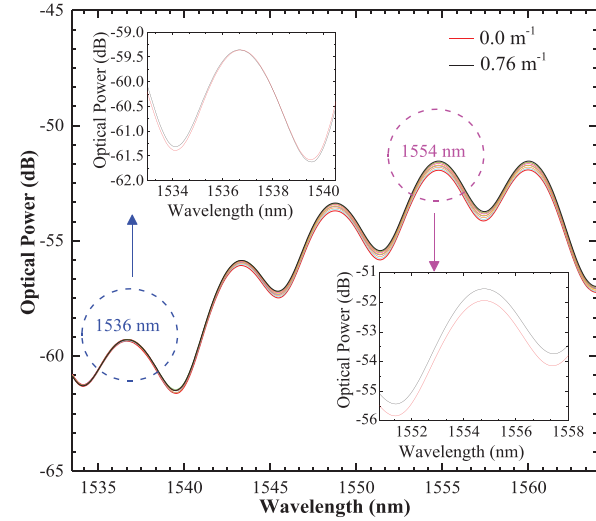


Fig. 2. Reflection spectra of FP cavity (inset: zoom in, in the insensitive region of the spectrum at 1536 nm, and in a highly sensitive region of the spectrum at 1554 nm).

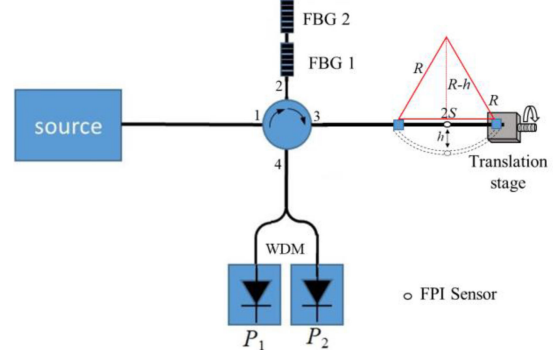


Fig. 3. Layout of the experimental setup used for self-referencing application.

FBGs (FBG 1 at 1536 nm and FBG 2 at 1554 nm) are placed in port 2. The objective is to create two discrete optical sources in two distinct regions of the FPI spectrum.

The FPI sensor is connected in port 3, and port 4 receives the reflection of the two FBGs modulated by the optical power variation of the FPI cavity. The optical power of the two FBGs is separated by a coarse wavelength division multiplexer with a spacing of 20 nm. Moreover, P_1 , P_2 are the optical powers measured at the insensitive and sensitive spectral regions of the FPI, respectively.

The spectral characteristic of this sensor allows the absolute value to be calculated for the measures of curvature and radius of curvature. For this, it will be necessary later to calculate the difference between P_2 and P_1 . First, by performing individual analysis of the curvature measurements of the two regions of interest, the results shown in Fig. 4 are obtained. Considering P_1 and P_2 as the optical power measured at the insensitive and sensitive spectral regions, respectively, it can be noted that for P_1 , the sensor has a residual sensitivity to curvature ($0.052 \pm 0.037 \text{ dB/m}^{-1}$), while for P_2 , a maximum sensitivity of $0.614 \pm 0.021 \text{ dB/m}^{-1}$ is achieved, with a correlation factor up to 0.989.

Also, a study was conducted relating the optical power and the radius of curvature for the same spectral regions presented above. The results are shown in Fig. 5. Once again, as in the curvature study,

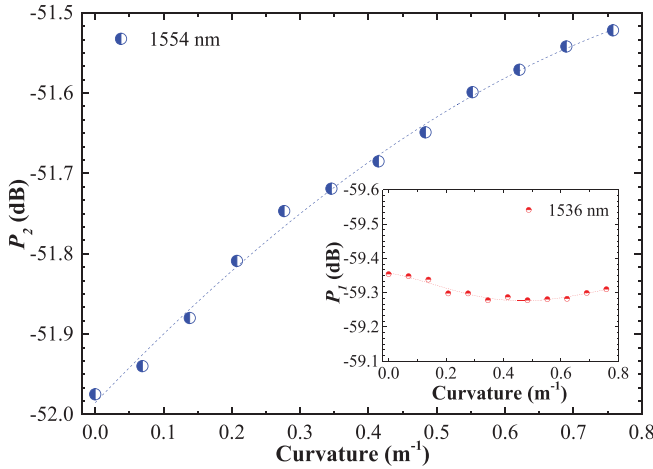


Fig. 4. Curvature measurements obtained in the studied spectral regions.

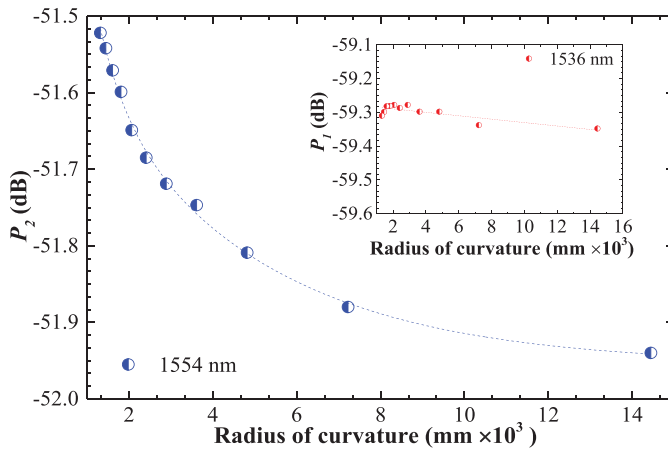


Fig. 5. Radius of curvature attained in the studied spectral regions.

the results for P_1 are negligible, whereas the results obtained for P_2 indicate that the sensor presents a nonlinear response for radius of curvature measurements, having higher sensitivity within the range between ~ 1319 and 4818 mm.

B. Self-Referencing Results

As already noted above for the self-referencing demonstration, an acquisition system, as shown on Fig. 3, was used.

On Fig. 6, it can be observed the absolute value for curvature and radius of curvature measurements. By analyzing them, it can be verified that there is an optical power shift towards longer optical powers. The dependence between the curvature response and the difference $P_2 - P_1$ presents a higher linear response, presenting a sensitivity of 0.561 ± 0.014 dB/m $^{-1}$, with a correlation factor up to 0.997.

The same analysis was made for the radius of curvature measurements. In the inset of Fig. 6, it was observed the absolute value for radius of curvature. The ideal range of operation of this sensor for this type of measurement is similar, which is shown in Fig. 5.

Considering the highest sensitivity obtained by the developed sensor and considering the acquisition system resolution, a maximum resolution of 0.018 m $^{-1}$ was estimated.

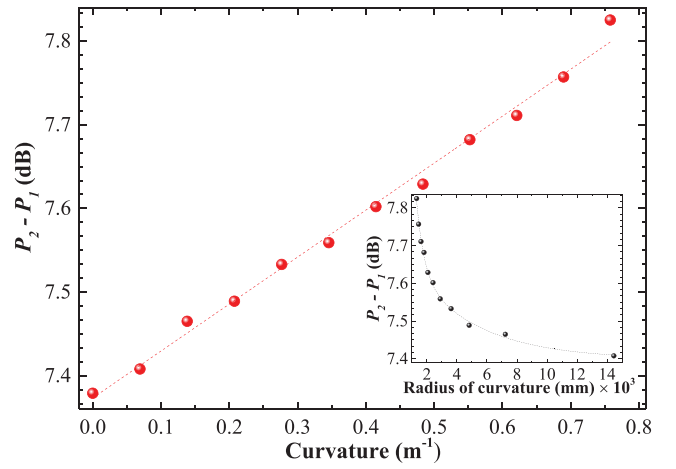


Fig. 6. Absolute value for curvature and for radius of curvature (inset) measurements.

Table 1. Comparison Between the Results Reported in Literature and This Work

Ref.	Configuration	Range (m^{-1})	Sensitivity
[15]	Single-mode fiber (SMF) + ceramic tube and double-cladding fiber	$0.71 - 1.18$	2554.53 pm/m $^{-1}$
[18]	Abrupt tapered fiber concatenated with a hollow core photonic crystal (HCPCF) + SMF	$0 - 3.5$	11.27 dB/m $^{-1}$
[11]	SMF+ capillary silica + SMF	$45 - 45$	17.27 pm/m $^{-1}$
[3]	SMF + HCPCF	$0 - 120$	0.30 dB/m $^{-1}$
[14]	SMF + hollow core fiber (HCF)	$0.7565 - 3.423$	5.05 dB/m $^{-1}$
[19]	SMF + no core fiber (NCF) + HCF	$0.8844 - 1.0995$	9.57 dB/m $^{-1}$
[20]	Eccentric-core fiber + HCF + MMF	$0 - 8.85$	79.50 pm/m $^{-1}$
This work	MMF + MMF*	$0 - 0.8$	0.56 dB/m $^{-1}$

*Self-referencing.

The temperature response of the proposed sensor was also experimentally investigated and demonstrated within the temperature range of 10 °C to 100 °C with a step of 10 °C.

The results show that the sensor exhibited a low thermal dependence, approximately 0.005 ± 0.02 dB/°C. This was somewhat expected since the temperature variation does not change the MMF-SMF launching conditions. The results are determined by the temperature dependence of the refractive index and the thermal expansion of the air bubble, which has typically a low dependency to temperature variation. Calculating the cross-sensitivity between the temperature and curvature, a value of 0.008 m $^{-1}/$ C was obtained.

The sensing device developed and presented in this work has several advantages. As the sensing structure is fabricated between two sections

of standard multimode fiber, the sensor is cost effective. Also, the acquisition system developed and its real-life application can be an advantage compared with others solutions presented in the literature. Notice that since it does not require any special fibers, this sensor can be an alternative to the sensors reported in the literature.

Table 1 shows a comparison between the results reported in the literature for curvature measurements and this work regarding FP interferometers.

IV. CONCLUSION

In conclusion, a self-referencing intensity-based fiber optic sensor to measure curvature is proposed and demonstrated experimentally. The curvature sensor is based on the principle of the Fabry–Perot interference, and by the analysis of two spectral fringes, where one fringe is insensitive to the applied curvature and the other is sensitive, it was possible to make a system of self-referencing and determine the absolute value of the measured parameter. After the analysis, an absolute value of $0.561 \pm 0.014 \text{ dB/m}^{-1}$ was obtained for curvature, with a maximum resolution of 0.018 m^{-1} . The temperature study was also carried out for the same sensor, and a residual sensitivity was achieved.

This sensor can be a good alternative to the bending sensors presented in the literature, as it is a simple sensor and also easy to manufacture. No special fibers, hazardous chemicals, or special techniques are required for their fabrication, and the proposed simple acquisition data system is an interesting solution for this type of measurements.

ACKNOWLEDGMENT

This work was supported in part by the ERDF – European Regional Development Fund through the Operational Programme for Competitiveness and Internationalization – COMPETE 2020 Programme and in part by National Funds through the Portuguese funding agency, FCT – Fundação para a Ciência e a Tecnologia within project ENDOR – Endoscope based on New Optical Fibre Technology for Raman Spectroscopy (POCI-01-0145-FEDER-029724).

REFERENCES

- [1] C. E. Lee, “Optical fiber Fabry–Perot sensors for smart structures,” *Smart Mater. Struct.*, vol. 1, no. 2, pp. 123–127, 1992.
- [2] M. Imai, T. Ohashi, and Y. Ohtsuka, “Multimode-optical-fiber michelson interferometer,” *J. Lightw. Technol.*, vol. 1, no. 1, pp. 75–8, 1983.
- [3] D. Jauregui-Vazquez *et al.*, “Highly sensitive curvature and displacement sensing setup based on all fiber micro Fabry–Perot interferometer,” *Opt. Commun.*, vol. 308, no. 1, pp. 289–292, 2013.
- [4] T. Yoshino, K. Kurosawa, K. Itoh, and T. Ose, “Fiber-optic Fabry–Perot interferometer and its sensor applications,” *IEEE Trans. Microw. Theory Technol.*, vol. MTT-30, no. 10, pp. 1612–1621, Oct. 1982.
- [5] S. Novais, M. Ferreira, and J. L. Pinto, “Optical fiber Fabry–Perot tip sensor for detection of water-glycerin mixtures,” *J. Lightw. Technol.*, vol. 36, no. 9, pp. 1576–1582, Sep. 2018.
- [6] A. Wang, H. Xiao, Z. Wang, W. Zhao, and R. G. May, “Self-calibrated interferometric-intensity-based optical fiber sensors,” *J. Lightw. Technol.*, vol. 19, no. 10, pp. 1495–1501, Oct. 2001.
- [7] S. Novais, M. S. Ferreira, and J. L. Pinto, “Lateral load sensing with an optical fiber inline microcavity,” *IEEE Photon. Technol. Lett.*, vol. 29, no. 17, pp. 1502–1505, Sep. 2017.
- [8] Y. Zhao, R. Lv, Y. Ying, and Q. Wang, “Hollow-core photonic crystal fiber Fabry–Perot sensor for magnetic fields measurement based on magnetic fluid,” *Opt. Laser Technol.*, vol. 44, no. 4, pp. 899–902, 2012.
- [9] L. A. Ferreira, A. B. Lobo Ribeiro, J. L. Santos, and F. Farahi, “Simultaneous measurement of displacement and temperature using a low finesse cavity and a fiber Bragg grating,” *IEEE Photon. Technol. Lett.*, vol. 8, no. 11, pp. 1519–1521, Nov. 1996. doi:[10.1109/68.541569](https://doi.org/10.1109/68.541569).
- [10] H. Gong, H. Song, X. Li, J. Wang, and X. Dong, “An optical fiber curvature sensor based on photonic crystal fiber modal interferometer,” *Sens. Actuators A, Phys.*, vol. 195, no. 6, pp. 139–141, 2013.
- [11] S. M. Catarina *et al.*, “Fiber Fabry–Perot interferometer for curvature sensing,” *Photon. Sens.*, vol. 6, no. 4, pp. 339–344, 2016.
- [12] C. Majidi, R. Kramer, and R. J. Wood, “A non-differential elastomer curvature sensor for softer-than-skin electronics,” *Smart Mater. Struct.*, vol. 20, no. 10, 2011, Art. no. 105017.
- [13] C. K. Y. Leung, K. T. Wan, and D. Inaudi, “Review: Optical fiber sensors for civil engineering applications,” *Mater. Struct.*, vol. 48, no. 4, pp. 871–906, 2018.
- [14] Y. Zhao, L. Cai, and X. Li, “In-fiber modal interference for simultaneous measurement of curvature and temperature based on hollow core fiber,” *Opt. Laser Technol.*, vol. 92, pp. 138–141, 2017.
- [15] X. Fu *et al.*, “A double-cladding fiber curvature sensor based on the extrinsic Fabry–Perot interferometer,” *Optoelectron. Lett.*, vol. 15, no. 1, pp. 6–10, 2019.
- [16] Q. Wang and W. M. Zhao, “A comprehensive review of lossy mode resonance-based fiber optic sensors,” *Opt. Lasers Eng.*, vol. 100, pp. 47–60, 2018.
- [17] J. Chen, P. Lu, and D. Liu, “Optical fiber curvature sensor based on few mode fiber,” *Optik*, vol. 125, no. 17, pp. 4776–4778, 2014.
- [18] M. Cano-Contreras, A. D. Guzman-Chavez, R. I. Mata-Chavez, E. Vargas-Rodriguez, D. Jauregui-Vazquez, and D. Claudio-Gonzalez, “All-fiber curvature sensor based on an abrupt tapered fiber and a Fabry–Pérot interferometer,” *IEEE Photon. Technol. Lett.*, vol. 26, no. 22, pp. 2213–2216, Nov. 2014.
- [19] Y. Wu, Y. Jiang, Y. Shen, L. Liang, Y. Yang, and S. Jian, “Simultaneous measurement of curvature and temperature based on asymmetrical FPI,” *IEEE Photon. Technol. Lett.*, vol. 29, no. 10, pp. 838–841, May 2017.
- [20] J. Kong, A. Zhou, and L. Yan, “Temperature insensitive one-dimensional bending vector sensor based on eccentric core fiber and air cavity Fabry–Perot interferometer,” *J. Opt.*, vol. 19, 2017, Art. no. 045705.
- [21] Y. Gong, Y. Guo, Y.-J. Rao, T. Zhao, and T. Wu, “Fiber-optic Fabry–Pérot sensor based on periodic focusing effect of graded-index multimode fibers,” *IEEE Photon. Technol. Lett.*, vol. 22, no. 23, pp. 1708–1710, Dec. 2010.
- [22] D. Donlagic and B. Culshaw, “Propagation of the fundamental mode in curved graded index multimode fiber and its application in sensor systems,” *J. Lightw. Technol.*, vol. 18, no. 83, pp. 334–340, 2000.
- [23] D. Donlagic and M. Zavrsnik, “Fiber-optic microbend sensor structure,” *Opt. Lett.*, vol. 22, no. 11, pp. 837–839, 1997.
- [24] G. Fu, Y. Li, Q. Li, J. Yang, X. Fu, and W. Bi, “Temperature insensitive vector bending sensor based on asymmetrical cascading SMF-PCF-SMF structure,” *IEEE Photon. J.*, vol. 9, no. 3, Jun. 2017, Art. no. 7103114.